Integration of fiber-coupled high-Q SiN_x microdisks with atom chips

Paul E. Barclay,[a] Kartik Srinivasan, and Oskar Painter
Thomas J. Watson, Sr. Laboratory of Applied Physics, California Institute of Technology, Pasadena, California 91125

Benjamin Lev and Hideo Mabuchi
Norman Bridge Laboratory of Physics, California Institute of Technology, Pasadena, California 91125

(Received 1 June 2006; accepted 21 July 2006; published online 27 September 2006)

Micron scale silicon nitride (SiN_x) microdisk optical resonators are demonstrated with $Q=3.6\times10^6$ and an effective mode volume of $15(\lambda/n)^3$ at near-visible wavelengths. A hydrofluoric acid wet etch provides sensitive tuning of the microdisk resonances, and robust mounting of a fiber taper provides efficient fiber optic coupling to the microdisks while allowing unfettered optical access for laser cooling and trapping of atoms. Measurements indicate that cesium adsorption on the SiN_x surfaces significantly red detunes the microdisk resonances. Parallel integration of multiple (10) microdisks with a single fiber taper is also demonstrated. © *2006 American Institute of Physics*. [DOI: 10.1063/1.2356892]

Atom chip technology[1,2] has rapidly evolved over the last decade as a valuable tool in experiments involving the cooling, trapping, and transport of ultracold neutral atom clouds. During the same period there has been significant advancement in microphotonic systems[3] for the guiding and trapping of light in small volumes, with demonstrations of photonic crystal nanocavities capable of efficiently trapping light within a cubic wavelength[4] and chip-based silica microtoroid resonators[5] with photon lifetimes well over 10^8 optical cycles. Poised to significantly benefit from these developments is the field of cavity quantum electrodynamics (cavity QED),[6] in which strong interactions of atoms with light inside a resonant cavity can be used to aid in quantum information processing and in the communication and distribution of quantum information within a quantum network.[7] Integration of atomic and microphotonic chips[8–10] offers several advancements to the current state-of-the-art Fabry-Pérot cavity QED systems,[11] most notably a scalable platform for locally controlling multiple quantum bits and an increased bandwidth of operation. In this letter we demonstrate the suitability of silicon nitride (SiN_x) for high-Q, small mode volume microcavities resonant at near-visible wavelengths necessary for cavity QED with alkali atoms, and describe a robust mounting technique which enables the integration of a permanently fiber-coupled microdisk resonator with a magnetostatic atom chip.

In addition to the obvious benefits of the fabrication maturity of the silicon (Si)-silicon oxide (SiO_x) materials system, recent work has shown that high quality atom chips can be created from thermally evaporated gold metal wires on thin oxide coated Si wafers.[12] Integration with a SiN_x optical layer provides a path towards a monolithic atom-cavity chip with integrated atomic and photonic functionality. Indeed, owing to its moderately high index of refraction ($n\sim2.0–2.5$) and large transparency window ($6\ \mu m>\lambda>300$ nm),[13,14] SiN_x is an excellent material for the on-chip guiding and localization of light. The high refractive index of SiN_x makes possible the creation of a variety of wavelength scale microcavity geometries such as whispering-gallery[15,16] or planar photonic crystal structures,[17] with a small intrinsic radiation loss. Combined with a lower index SiO_x cladding, waveguiding in a SiN_x layer can be used to distribute light within a planar microphotonic circuit suitable for high-density integration. The low absorption loss across the visible and near-IR wavelengths, on the other hand, allows SiN_x to be used with a diverse set of atomic and atomiclike (colloidal quantum dots, color centers, etc.) species. Beyond the particular focus of this work on cavity QED experiments with cold alkali atoms, high-Q SiN_x microcavities are also well suited to experiments involving moderate refractive index environments, such as sensitive detection of analytes contained in a fluid solution[18] or absorbed into a low index polymer cladding.[19]

The SiN_x microdisk resonators in this work were fabricated from a commercially available Si wafer with a 250 nm thick stoichiometric SiN_x ($n=2.0$) layer grown on the surface by low pressure chemical vapor deposition (LPCVD). Fabrication of the microdisk resonators involved several steps, beginning with the creation of a highly circular electron beam resist etch mask through electron beam lithography and a resist reflow.[20] A C_4F_8/SF_6 plasma dry etch was optimized to transfer the resist etch mask into the SiN_x layer as smoothly as possible. This was followed by a potassium hydroxide wet etch to selectively remove the underlying $\langle100\rangle$ Si substrate until the SiN_x microdisks were supported by a small micron diameter silicon pillar. A final cleaning step to remove organic materials from the disk surface was performed using a $H_2SO_4:H_2O_2$ wet etch. A scanning electron microscope (SEM) image of a fully processed microdisk is shown in Figs. 1(a) and 1(b).

The optical modes of the fabricated microdisks were efficiently excited via an optical fiber taper waveguide.[21,22] A swept wavelength source covering the 840–856 nm wavelength band was coupled into the fiber taper waveguide and used to measure the transmission spectra of the microdisk resonators at wavelengths close to the D2 transition of cesium (Cs). Details of the fiber taper measurement setup can be found in Ref. 20. Figure 2(a) shows a typical measured wavelength scan of the lowest radial order ($p=1$) TE-like mode of a 9 μm diameter SiN_x microdisk. The resonance has

[a]Electronic mail: pbarclay@caltech.edu

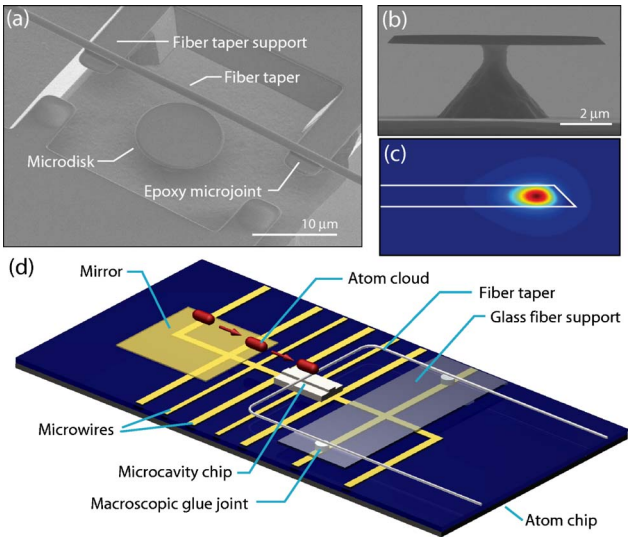

FIG. 1. (Color online) (a) Scanning electron microscope (SEM) image of a SiN_x cavity coupled to an optical fiber taper. The fiber taper is permanently aligned a few hundreds of nanometers from the microdisk circumference with epoxy microjoints to SiN_x supports. (b) Side-view SEM image of a 9 μm diameter mircodisk. (c) FEM calculated field distribution ($|E|^2$) of a $m=50$, $p=1$, TE-like mode of the microdisk in (b). (d) Schematic of the integrated hybrid atom-cavity chip.

an intrinsic linewidth of 0.26 pm, corresponding to a quality factor $Q=3.6\times10^6$. The doublet structure in the transmission spectra is due to mode coupling between the clockwise and counterclockwise modes of the disk due to surface roughness induced backscattering.[23] In addition to this high-Q mode, the 9 μm microdisks also support a lower Q higher-order radial mode in the 850 nm wavelength band. The free spectral range between modes of the same radial order but different azimuthal number (m) was measured to be 5.44 THz (13 nm), resulting in a finesse of $\mathcal{F}=5\times10^4$ for the $p=1$, TE-like modes. Tests of less surface sensitive larger diameter microdisks showed reduced doublet splitting but no reduction in linewidth, indicating that Q is most likely limited by material absorption and not surface roughness.[20] This bodes well for utilizing these SiN_x microdisks at even shorter wavelengths, such as the 780 nm D2 transition of rubidium.

Finite element method (FEM) simulations[20] [Fig. 1(c)] show that the effective optical mode volume, defined by $V_{\text{eff}}=\int n^2(\mathbf{r})E^2(\mathbf{r})d\mathbf{r}/|n^2(\mathbf{r})E^2(\mathbf{r})|_{\max}$, is 15 $(\lambda/n)^3$ for the 9 μm diameter mirodisks. The corresponding parameters of cavity QED, the Cs-photon coherent coupling rate (g), photon field decay rate (κ), and Cs transverse decay rate ($\gamma_\perp$), are $[g,\kappa,\gamma_\perp]/2\pi=[2.4,0.05,0.003]$ GHz for an atom at the mircodisk surface, indicating that these cavities are capable of operating well within the regime of strong coupling.[6] For an atom displaced 100 nm from the surface, $g/2\pi$ drops to 0.9 GHz. FEM simulations show that for microdisks of diameter below 9 μm the intrinsic radiation Q drops rapidly below the 10^8 level.

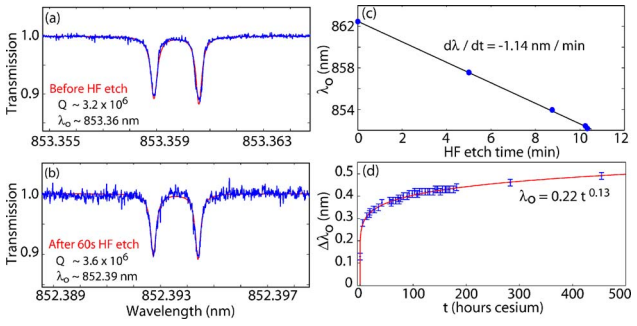

FIG. 2. (Color online) Wavelength scan of the fiber taper transmission for a $p=1$, TE-like mode of a 9 μm diameter SiN_x microdisk (a) prior to and (b) after HF wet etch tuning of the resonance wavelength. (c) Resonance wavelength (λ_o) of the $p=1$, TE-like mode of an 11 μm diameter microdisk as a function of HF etch time. (d) Shift in λ_o as a function of time exposed to cesium vapor (partial pressure $\sim10^{-9}$ Torr) in an UHV chamber.

Using the above fabrication procedure the resonance wavelength (λ_o) of the microdisk modes could be positioned with an accuracy of ±0.5 nm. In order to finely tune λ_o into alignment with the D2 atomic Cs transition a series of timed etches in 20:1 diluted 49% HF solution was employed. By slowly etching the LPCVD SiN_x the resonance wavelength of the high-Q disk modes was shown to blueshift at a rate of 1.1 nm/min [Fig. 2(c)]. With this technique the cavity resonance could be positioned with an accuracy of ±0.05 nm without degrading the Q factor [Fig. 2(b)]. Further fine-tuning can be accomplished by heating and cooling of the sample; a temperature dependence of $d\lambda_o/dT\sim0.012$ nm/°C was measured for the $p=1$, TE-like microdisk modes.

After initial device characterization and tuning of λ_o, the fiber taper and microdisk chip were integrated with an atom chip consisting of a sapphire substrate with electroplated gold microwires underneath a top evaporated gold mirror layer.[8,24] A brief outline of the integration procedure follows. The $3\times3\times0.3$ mm^3 Si microcavity chip is aligned and bonded to the desired location on the top surface of the atom chip using polymethyl methacrylate. The fiber taper is supported in a self-tensioning "U" configuration by a glass coverslip (~200 μm thick), as illustrated in Fig. 1(d). The taper is aligned with the microdisk using dc motor stages with 50 nm encoder resolution. Adjustment of the lateral gap between the taper and the microdisk is used to tune the level of cavity loading; owing to the excellent phase matching of the fiber taper guided mode to the whispering-gallery modes of the microdisk[22] critical coupling was possible with a loaded $Q\sim10^6$. The fiber taper and microdisk are then permanently attached using UV curable epoxy in two regions: (i) microscopic glue joints between the fiber taper and lithographically defined SiN_x supports [see Fig. 1(a)] fix the position of the taper relative to the disk, and (ii) macroscopic glue joints between the taper support slide and the atom chip [see Fig. 1(d)] fix the position of the taper support relative to the chip and serve as stress relief points for the fiber pigtails. To avoid blocking trapping laser beams or obscuring imaging, the entire fiber taper mount must lie below the plane of the optically and magnetically trapped atoms (~600 μm above the atom chip surface). A sufficiently low profile is achieved by aligning and bonding the taper support glass coverslip parallel to and below the plane of the microdisk chip top surface. During the taper mounting procedure the taper-microdisk coupling is monitored by measuring λ_o and the transmission contrast (ΔT), with no noticeable change being observed during the curing of the epoxy joints. The microglue joints incur a taper diameter dependent amount of broadband insertion loss; for the taper diameters used here (~1 μm) an approximate 10%–15% optical loss per joint is typical. Postcure, the fiber-cavity alignment is extremely robust, withstanding all of the vacuum installation procedures described below.

The integrated atom-cavity chip was installed in an ultrahigh vacuum (UHV) chamber designed for performing atom chip waveguiding experiments. Vacuum-safe fiber feedthroughs[25] were used to pass the fiber pigtails out of the chamber. The chamber was evacuated using turbo and ion pumps and baked at 130 °C for 24 h so that a background pressure of $<10^{-8}$ Torr was reached. Initial experiments with the integrated system involved the trapping of Cs atoms in a mirror-MOT (magneto optical trap)[1] above the atom chip gold mirror and transfer of atoms to a micro-U-MOT (Ref. 1) for subsequent magnetic trapping and guiding on the atom chip [see Fig. 1(d)]. The extremely low profile of the fiber taper mounting was shown to provide excellent optical access for atom trapping, cooling, and imaging. The microdisk resonance was continuously monitored during these procedures. ΔT was found to remain constant during the chamber pump down, bakeout, and atom trapping, demonstrating the robustness of the fiber-cavity mounting. However, after the chamber bake, λ_o was redshifted 0.11 nm from the prebake value and was found to increase logarithmically with exposure time to the Cs vapor, as shown in Fig. 2(d). During subsequent chamber bakes and intermittent closures of the Cs source (for periods as long as two weeks) λ_o was found to remain constant.

The logarithmic time dependence of λ_o with Cs exposure suggests that the Cs coverage of the microdisk surface is saturating in a "glassy" manner;[26] interactions between deposited atoms quench the rate of adsorption. A shift $\Delta\lambda_o$ of the disk resonances can be related to a surface film thickness by $s \sim \Delta\lambda_o/(\lambda_o(n_f-1)\Gamma')$, where $\Gamma' s$ represents the fraction of modal energy in the film and n_f is the refractive index of the film. From finite element simulations of the microdisk, $\Gamma'=0.0026\ \mathrm{nm}^{-1}$ for the $p=1$, TE-like mode. Assuming a film index of refraction equal to that of SiN_x, the measured wavelength shift at the longest measured time ($t=450$ h) corresponds to roughly a half-monolayer coverage of Cs on the disk surface [monolayer thickness ~4 Å] (Ref. 27).

As a future method of compensating for resonant detuning of the microdisk mode due to variation in fabrication or the time-dependent Cs surface coverage, and as an initial demonstration of the scalability of the fiber-coupled microdisk chip concept, we show in Fig. 3(a) a single fiber taper coupled in parallel to an array of ten nominally identical microdisks [Fig. 3(b)]. Over a ±0.25 nm wavelength range the fiber taper couples to 5 of the $p=1$, TE-like modes as shown in Fig. 3(c), the remaining five modes lying within a ±1 nm range. A modest 10 °C of temperature tuning may be used to tune between the five closely spaced modes. Each of these resonances is due to coupling to a unique microdisk, as verified by imaging the scattered light from the microdisks as a function of wavelength.

In conclusion, we have shown that wavelength scale high-Q microcavities can be realized from SiN_x at near-visible wavelengths and have demonstrated a method for integrating these devices with atom chips. The resulting optical fiber taper interface to the hybrid atom-cavity chip provides sufficient optical access for chip-based atom trapping and cooling while providing highly efficient optical coupling to single, or simultaneously to multiple, microdisk cavities. In the future, the use of SiN_x microcavities provides a path to a fully monolithic atom-cavity Si chip.

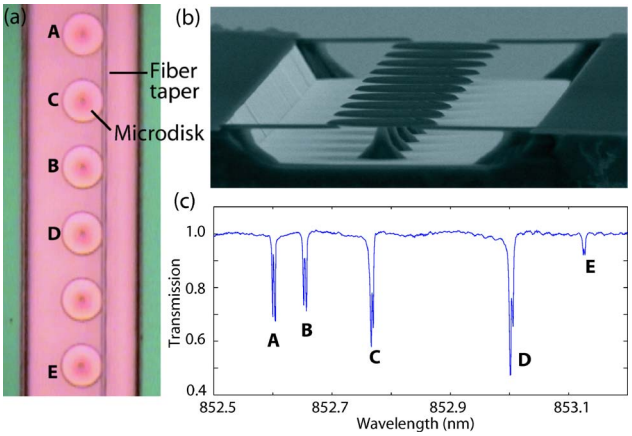

FIG. 3. (Color online) (a) Top-view optical image of a fiber taper aligned with and array of ten microdisks (the remaining four microdisks are out of the field of view of the image). (b) SEM image of the array of ten microdisks. (c) Fiber taper transmission vs wavelength when the taper is aligned with the microdisk array in (a). The letters match specific microdisks in (a) with the corresponding resonances in (c).

The authors thank M. Borselli and T. Johnson for assistance in FEM simulations and microdisk process development, and J. Kerckhoff for help with Cs adsorption measurements.

[1] J. Reichel, Appl. Phys. B: Lasers Opt. **74**, 469 (2002).
[2] R. Folman, P. Krüger, J. Schmiedmayer, J. Denschlag, and C. Henkel, Adv. At., Mol., Opt. Phys. **48**, 263 (2002).
[3] K. J. Vahala, Nature (London) **424**, 839 (2003).
[4] B.-S. Song, S. Noda, T. Asano, and Y. Akahane, Nat. Mater. **4**, 207 (2005).
[5] D. K. Armani, T. J. Kippenberg, S. M. Spillane, and K. J. Vahala, Nature (London) **421**, 925 (2003).
[6] H. J. Kimble, Phys. Scr., T **T76**, 127 (1988).
[7] L. M. Duan and H. J. Kimble, Phys. Rev. Lett. **92**, 127902 (2004).
[8] B. Lev, K. Srinivasan, P. E. Barclay, O. Painter, and H. Mabuchi, Nanotechnology **15**, S556 (2004).
[9] A. Haase, B. Hessmo, and J. Schmiedmayer, Opt. Lett. **31**, 268 (2006).
[10] M. Rosenblit, P. Horak, S. Helsby, and R. Folman, Phys. Rev. A **70**, 053808 (2004).
[11] J. McKeever, A. Boca, A. D. Boozer, R. Miller, J. R. Buck, A. Kuzmich, and H. J. Kimble, Science **303**, 1992 (2004).
[12] S. Groth, P. Krüger, S. Wildermuth, R. Folman, T. Fernholz, J. Schmiedmayer, D. Mahalu, and I. Bar-Joseph, Appl. Phys. Lett. **85**, 2980 (2004).
[13] G. N. Parsons, J. H. Souk, and J. Batey, J. Appl. Phys. **70**, 1553 (1991).
[14] T. Inukai and K. Ono, Jpn. J. Appl. Phys., Part 1 **33**, 2593 (1994).
[15] B. E. Little, S. T. Chu, P. P. Absil, J. V. Hryniewicz, F. Seiferth, D. Gill, V. Van, O. King, and M. Traklo, IEEE Photonics Technol. Lett. **16**, 2263 (2004).
[16] T. Barwicz, M. A. Popovic, P. T. Rakich, M. R. Watts, H. A. Haus, E. P. Ippen, and H. I. Smith, Opt. Express **12**, 1437 (2004).
[17] M. C. Netti, M. D. B. Charlton, G. J. Parker, and J. J. Baumberg, Appl. Phys. Lett. **76**, 991 (2000).
[18] F. Vollmer, D. Braun, A. Libchaber, M. Khoshsima, I. Teraoka, and S. Arnold, Appl. Phys. Lett. **80**, 4057 (2002).
[19] A. Ksendzov, M. L. Homer, and A. M. Manfreda, Electron. Lett. **40**, 63 (2004).
[20] M. Borselli, T. J. Johnson, and O. Painter, Opt. Express **13**, 1515 (2005).
[21] J. Knight, G. Cheung, F. Jacques, and T. Birks, Opt. Lett. **22**, 1129 (1997).
[22] S. M. Spillane, T. J. Kippenberg, O. J. Painter, and K. J. Vahala, Phys. Rev. Lett. **91**, 043902 (2003).
[23] T. J. Kippenberg, S. M. Spillane, and K. J. Vahala, Opt. Lett. **27**, 1669 (2002).
[24] B. Lev, Quantum Inf. Comput. **3**, 450 (2003).
[25] R. I. Abraham and E. A. Cornell, Appl. Opt. **37**, 1762 (1998).
[26] R. G. Palmer, D. L. Stein, E. Abrahams, and P. W. Anderson, Phys. Rev. Lett. **53**, 958 (1984).
[27] M. Brause, D. Ochs, J. Günster, T. Mayer, B. Braun, V. Puchin, W. Maus-Friedrichs, and V. Kempter, Surf. Sci. **383**, 216 (1997).